PYROELECTRIC AND D.C. RESISTIVITY STUDIES OF BARIUM STRONTIUM CERIUM LITHIUM SODIUM NIOBATE CERAMICS

CHANDRAMOULI K., VISWARUPACHARY P., RAMAM KODURI*

*Solid State Physics and Materials Research Laboratory, Department of Physics,
Andhra University, Visakhapatnam, India
* Departmento de Ingenieria de Materiales, (DIMAT), Facultad de Ingenieria,
Universidad de Concepcion, Concepcion, Chile*

E-mail: ramamk@udec.cl

$Ba_{1.45}Sr_{2.4}Ce_{0.1}LixNa_{2-x}Nb_{10}O_{30}$ ceramic compositions in the range of x = 0.0 ≤ x ≤ 1.0, which belong to tungsten-bronze structural family were prepared using a solid-state reaction technique. X-ray diffraction study confirms the formation of the compounds in an orthorhombic tungsten bronze (mm^2, OTB) phase at room temperature which has been supported by tolerance factor and average electronegativity difference. Measurement of conductivity as a function of temperature suggests that the samples have positive temperature coefficient of resistance (PTCR) with typical semiconductor behavior which could be suitable for pyroelectric and PTCR applications. The pyroelectric properties of BSCLNN – Barium Strontium Cerium Lithium Sodium Niobate ceramics are reported.

INTRODUCTION

Barium strontium sodium niobate $(Ba_{1-x}Sr_x)_2Na Nb_5O_{15}$ [BSNN] is a ferroelectric material that has a tungsten bronze type structure [1]. In recent years ferroelectric materials of tungsten-bronze (TB) family have received considerable interest because of their growing use in electronic, electro-optical, optical, acoustic, microwave etc. devices [2]. A wide variety of applications of BSNN-based materials include integrated non-volatile and dynamic random access memories, pyroelectric detectors, optical storage medium, delay lines, acoustic transducers and microwave resonators as well as phase shifters [3].

$K_3Li_{2-x}Nb_{5+x}O_{15+x}$ (KLN) and Ce:Nd:KLN crystals (the starting composition for KLN was the mixture of Nb_2O_5:K_2CO_3:Li_2CO_3 = 47.7%:35%:17.3%, the amount of Nd_2O_3 and Ce_2O_3 = 0.1 % and 0.08 %, respectively) were grown by Czochralski method for photorefractive properties [4]. $Ba_pNd_{6-p}Ti_{8-p}Nb_{2+p}O_{30}$ system was prepared, and their microstructures were evaluated together with the dielectric characterization and the effect of different ions in the A and B sites [5]. Most of these applications exploit the properties of the ferroelectric phase. A number of ferroelectric compounds having TB structure such as $(Sr,Ba)Nb_2O_6$ [6, 7], $(Pb,Ba)Nb_2O_6$ [8], rare-earth doped $(Sr,Ba)Nb_2O_6$ [9], $Pb_2Bi_4Ti_5O_{18}$ [10], $(Pb,K)LiTa_{10}O_{30}$ [1], $Ba_2NaNb_5O_{15}$ [11], $Ba_2Na_3RNb_{10}O_{30}$ (R = rare-earth ions) [12], $Ba_5RTi_3Nb_7O_{30}$ (R Dy, Sm) [13], (R Nd, Eu, Gd) [14], $Ba_4R_2Ti_4Nb_6O_{30}$ (R Y, Sm, Dy) [15], $Ba_5Nd(Ti,Zr)Nb_7O_{30}$ [16], etc. have been extensively investigated for intended applications. These multi-component systems are very sensitive to the additives and show variety of phase transitions. Furthermore, tungsten bronze niobates [17] have been found to show promising dielectric properties.

An extensive literature survey suggested that there are no reports available regarding the study of Lithium-modified and Cerium-doped $Ba_{1.6}Sr_{2.4}Na_2Nb_{10}O_{30}$ tungsten bronze ceramic system. Accordingly in the present work, to the best knowledge of the author for the first time we report the influence of alkali Lithium modified on Cerium doped BSNN tungsten bronze ceramic system for pyroelectric and D.C. Resistivity studies are reported. The stoichiometric compositions synthesized are represented in Table 1.

EXPERIMENTAL

Analytical reagent grade powders (purity 99.9 %) $BaCO_3$, $SrCO_3$, Na_2CO_3, Li_2CO_3, Nb_2O_5 and Ce_2O_3 were used as starting materials and the solid solutions were prepared by the solid-state reaction method. The batch powders were ball milled using zirconia balls with ethanol as the medium, for 24 h and dried. These powders were calcined at 950°C for 6 h in a platinum crucible in air. The calcined fine powders were then mixed with 5 wt.% polyvinyl alcohol as binder and pressed into pellets of 15 mm diameter and 2 mm thickness using steel die and a hydraulic press with a uniaxial pressure of 5 tonnes per sq. inch. The binder was burned off at 600°C in the green bodies and then sintered at 1250°C for 6 h. The phase genesis of sintered specimens

was characterized by Philips X'pert diffractometer (Cuk$_\alpha$ radiation, λ = 1.5405 Å). The polished ceramic surfaces were silver-electroded and characterized for temperature dependent pyroelectric properties. The pyroelectric response was measured by using Keithley Electrometer Model 614 and microprocessor 8085 based temperature controlled furnace. A constant voltage of 10 V/cm was applied across the sample to measure D.C. resistivity by a two terminal method.

RESULTS AND DISCUSSION

Phase analysis of Ce doped BSLNN ceramics

Figure 1 shows X-ray diffraction patterns of BSCLNN ceramics. All the samples exhibit a single-phase orthorhombic (mm^2) crystal structure. The tungsten bronze A_2BC_2 (M'_4M'')O_4 ($M' = M'' = Nb$) oxides can be described by a framework of MO_6 octahedra sharing groups, delimiting tunnels of pentagonal, square and triangular sections. The sites of pentagonal coordination 15 (A2-site) and square coordination 12 (A1-site) are usually occupied by large size cations. On the other hand, cations of small size occupy in the triangular sites of 9-fold coordination. In our study, it is speculated that in the orthorhombic BSNN tungsten bronze filled-structure, Ba^{2+} (1.61 Å) could occupy the A2-site i.e. 15-coordinated-pentagon and Sr^{2+} (1.44 Å), Na^+ (1.24 Å), Ce^{3+} (1.34 Å) and Li^+ (0.92 Å) could occupy A1-site i.e. 12-coordinated-square and Nb^{5+} (0.74 Å) could occupy B-site i.e. 6-coordinated-diamond while the C-site is occupied by small cations or empty. Sr^{2+} is occupying mainly so-called A1 sites, whereas Ba^{2+} prefers the A2 sites. The cerium ion in BSLNN is found dominantly in a trivalent charge state (> 90 %) and occupies preferentially in Sr^{2+} sites. The maximum axial ratio ($\sqrt{10}c/a$ = 0.7003) is obtained in the composition in

$Ba_{1.45}Sr_{2.4}Ce_{0.1}Li_{0.8}Na_{1.2}Nb_{10}O_{30}$ while maximum unit cell volume (1203.79 Å^3) in $Ba_{1.45}Sr_{2.4}Ce_{0.1}Li_{0.4}Na_{1.6}Nb_{10}O_{30}$. The value of lattice parameters varies with the increasing content of Lithium influencing the unit cell volume.
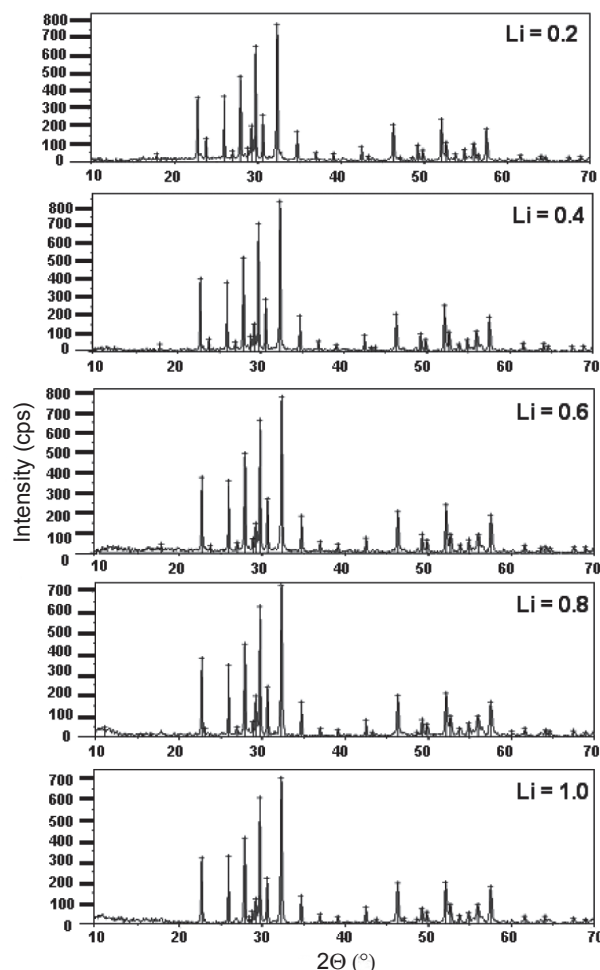
Figure 1. X-ray diffraction patterns of BSCLNN ceramics.

Table 1. Stoichiometric Compositions of BSCLNN solid solutions.

Composition	Formulae
BSNN + Ce$_y$ + Li$_x$	(1.6-[3/2]y)BaCO$_3$ + 2.4SrCO$_3$ + (y/2)Ce$_2$O$_3$ + (x/2)Li$_2$CO$_3$ + ([2-x]/2)Na$_2$CO$_3$ + 5Nb$_2$O$_5$ → → Ba$_{1.6-(3/2)y}$Sr$_{2.4}$Ce$_y$Li$_x$Na$_{(2-x)}$Nb$_{10}$O$_{30}$ + (5-[3/2]y)CO$_2$↑
BSNN + Ce$_{0.1}$ + Li$_x$	1.45BaCO$_3$ + 2.4SrCO$_3$ + 0.05Ce$_2$O$_3$ + (x/2)Li$_2$CO$_3$ + ([2-x]/2)Na$_2$CO$_3$ + 5Nb$_2$O$_5$ → → Ba$_{1.45}$Sr$_{2.4}$Ce$_{0.1}$Li$_x$Na$_{(2-x)}$Nb$_{10}$O$_{30}$ + 4.85CO$_2$↑
x = 0.2	1.45BaCO$_3$ + 2.4SrCO$_3$ + 0.05Ce$_2$O$_3$ + 0.1Li$_2$CO$_3$ + 0.9Na$_2$CO$_3$ + 5Nb$_2$O$_5$ → → Ba$_{1.45}$Sr$_{2.4}$Ce$_{0.1}$Li$_{0.2}$Na$_{1.8}$Nb$_{10}$O$_{30}$ + 4.85CO$_2$↑
x = 0.4	1.45BaCO$_3$ + 2.4SrCO$_3$ + 0.05Ce$_2$O$_3$ + 0.2Li$_2$CO$_3$ + 0.8Na$_2$CO$_3$ + 5Nb$_2$O$_5$ → → Ba$_{1.45}$Sr$_{2.4}$Ce$_{0.1}$Li$_{0.4}$Na$_{1.6}$Nb$_{10}$O$_{30}$ + 4.85CO$_2$↑
x = 0.6	1.45BaCO$_3$ + 2.4SrCO$_3$ + 0.05Ce$_2$O$_3$ + 0.3Li$_2$CO$_3$ + 0.7Na$_2$CO$_3$ + 5Nb$_2$O$_5$ → → Ba$_{1.45}$Sr$_{2.4}$Ce$_{0.1}$Li$_{0.6}$Na$_{1.4}$Nb$_{10}$O$_{30}$ + 4.85CO$_2$↑
x = 0.8	1.45BaCO$_3$ + 2.4SrCO$_3$ + 0.05Ce$_2$O$_3$ + 0.4Li$_2$CO$_3$ + 0.6Na$_2$CO$_3$ + 5Nb$_2$O$_5$ → → Ba$_{1.45}$Sr$_{2.4}$Ce$_{0.1}$Li$_{0.8}$Na$_{1.2}$Nb$_{10}$O$_{30}$ + 4.85CO$_2$↑
x = 1.0	1.45BaCO$_3$ + 2.4SrCO$_3$ + 0.05Ce$_2$O$_3$ + 0.5Li$_2$CO$_3$ + 0.5Na$_2$CO$_3$ + 5Nb$_2$O$_5$ → → Ba$_{1.45}$Sr$_{2.4}$Ce$_{0.1}$Li$_{1.0}$Na$_{1.0}$Nb$_{10}$O$_{30}$ + 4.85CO$_2$↑

The increase in the unit cell volume could be due to the substitution of Li in lower concentrations as Li has less ionic radius when compared to the other elements in the lattice. It is observed that there is a variation in the unit cell volume at higher concentrations of Li due to the ionic radii of multiple dopants in A1-site, i.e. (12-coordinated-square. The XRD indicates that dopants have entered the lattice by substitution perfectly and there is no distortion in the single-phase orthorhombic (mm^2) crystal structure. Figure 2 illustrates Tungsten Bronze BSCLNN system. It is observed that Ce^{3+} substitutes Ba^{2+} at A2-site while Li$^+$ substitutes both Sr^{2+} and Na$^+$ at A1-site in the BSCLNN tungsten bronze system. Thus, BSCLNN ceramics has an orthorhombic crystal structure which is comparable with the literature [18]. These substitutions influenced the lattice parameters along with the unit cell volume. The rare-earth Ce^{3+} and alkali Li$^+$ influence on BSNN could be attributed to the difference in the ionic radii of the cations, respectively. In the present investigation, the average linear particle size for all compositions have been calculated from XRD data and reflection peaks, which are widely scattered in the 2θ range ($10° \leq 2θ \leq 70°$). The results of average particle size and XRD data indicate orthorhombic monophase constitution in BSNLNN ceramic system.

We have discussed the formulae of tolerance factor and averaged electronegativity difference in our previous studies [19]. By using the general formula for the present tungsten bronze compounds, the averaged electronegativity difference (e) can be written as:

$$e = \frac{\{((1.6-(3/2)y)\chi_{Ba-O} + 2.4\chi_{Sr-O} + y\chi_{Ce-O} + x\chi_{Li-O} + (2-x)\chi_{Na-O} + 10\chi_{Nb-O})\}}{((32-y)/2)}$$
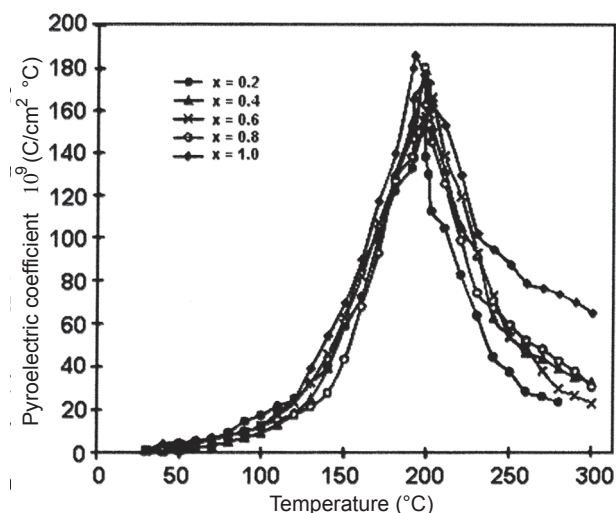
Figure 3. Temperature dependent pyroelectric response of BSCLNN ceramics.

Table 2. Lattice Parameters, unit cell volume, axial ratio, particle size and density of BSCLNN solid solutions.

| Li | Lattice Parameters | | | Unit cell volume (Å)^3 | Axial ratio ($\sqrt{10}\,c/a$) | Particle size (Å) | Density (gm/cm^3) | Tolerance factor (t) | Avg. Electronegativity difference (e) |
	a (Å)	b (Å)	c (Å)						
Li$_{0.2}$	17.5119	17.6314	3.8722	1195.57	0.6992	265	4.72	0.6426	2.0894
Li$_{0.4}$	17.5253	17.7431	3.8713	1203.79	0.6985	243	4.61	0.6420	2.0887
Li$_{0.6}$	17.5300	17.5900	3.8700	1193.32	0.6981	241	4.60	0.6414	2.0881
Li$_{0.8}$	17.4803	17.7433	3.8716	1200.80	0.7003	250	4.55	0.6408	2.0875
Li$_{1.0}$	17.4893	17.6268	3.8711	1193.38	0.7000	287	4.69	0.6402	2.0869
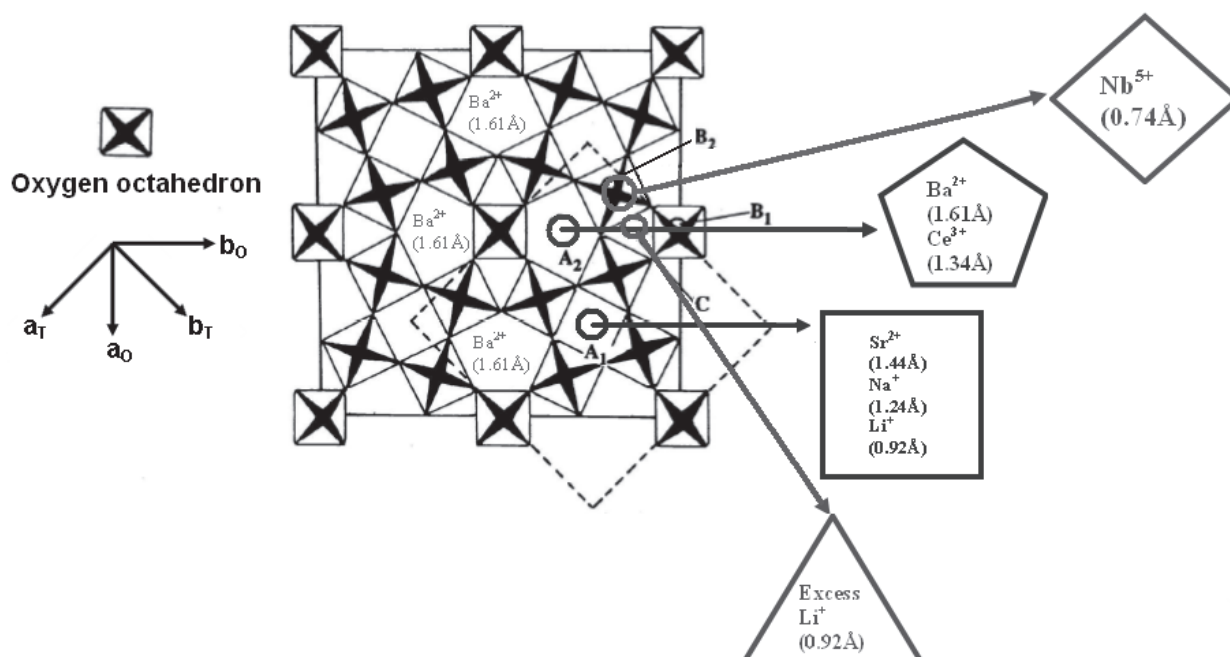
Figure 2. Tungsten Bronze BSCLNN system.

The lattice parameters, unit cell volume, axial ratios, average particle size, tolerance factor and electronegativity difference are given in Table 2. It is evident that BSCLNN adopts a stable orthorhombic phase. Hence, it can be justified that the multiple dopants constituted perfect orthorhombic (mm²) structure.

Pyroelectric properties of Ce doped BSLNN ceramics

Figure 3 indicates the temperature dependent pyroelectric response of BSCLNN ceramics. The pyroelectric coefficients has been calculated from the general formula as $P = dp/dt$, where dp is the change in polarization and dt is temperature change. The quality of the pyroelectric materials can be evaluated through different figures of merits. The formulae of the figure of merits are:

I. Voltage responsivity, $FM_{RV} = \dfrac{P}{\rho\, Cp\, K}$ (1)

II. Normalized detectivity, $FM_{RN} = \dfrac{P}{\rho\, Cp\, \sqrt{K}}$ (2)

III. Current responsivity, $FM_{RI} = \dfrac{P}{\rho\, Cp}$ (3)

where Cp is the specific heat.

The values of P_{RT} increase from 0.92×10^{-9} C/cm² per °C to 1.21×10^{-9} C/cm² per °C with increase of Li⁺ concentration except at 0.4 Li⁺ concentration. The P_{max} values also increase from 1.51×10^{-7} C/cm² per °C to 1.85×10^{-7} C/cm² per °C with increase of Li⁺ concentration except at 0.4 Li⁺ content in the Ce-BSLNN composition. It is clear from the figure that pyroelectric behavior in Ce-BSLNN complies with our earlier studies in BSLNN, Dy-BSLNN, Sm-BSLNN and Nd-BSLNN materials. There are two orders of magnitude rise in the values of pyroelectric coefficient (P_{max}) at P_{Tc} compared with P_{RT}. The value of P_{RT} in Ce doped BSLNN is found in the order of 10^{-9} C/cm² per °C. A similar behavior has been found in rare-earth ion substituted in barium strontium sodium niobate ceramic materials [20]. The figures of merit FM_{RV}, FM_{RN} and FM_{RI} have been calculated and these values are in the order of 10^{-14}, 10^{-12} and 10^{-11} CM/J, respectively. These values are only one order

of magnitude less when compared with the same values obtained in similar compounds of TB-type rare-earth ions doped BSLNN pyrocrystalline ceramics. The maximum P_{RT}, P_{max} with optimum P_{Tc} has been observed in $Li_{1.0}$. The optimum figure of merit of voltage responsivity ($FM_{RV} = 1.86\times10^{-14}$ CM/J) has been observed in $Li_{0.6}$, normalized detectivity ($FM_{RN} = 0.35\times10^{-12}$ CM/J) has been observed in $Li_{0.6}$ and current responsivity ($FM_{RI} = 0.78\times10^{-11}$ CM/J) has been observed in $Li_{1.0}$, respectively. The values of P_{RT}, P_{max}, P_{Tc}, FM_{RV}, FM_{RN} and FM_{RI} are given in Table 3.

D.C. Resistivity of Ce doped BSLNN ceramics

Temperature variation of resistivity Li⁺ modified with rare-earth ion Ce³⁺ doped BSLNN ceramic materials are shown in Figure 4. In accordance with the two terminal method, the flow of current through the circuit, voltage across the sample, and resistivity of the sample could be calculated by using the following formula:

$$\rho = \frac{RA}{l}\ \Omega\text{cm}$$ (4)

where R is the resistance of the sample, $A = \pi r^2$, surface area, r is radius of the sample, l is the thickness of the sample and ρ is the resistivity of the sample. The activation energies of the samples are estimated from
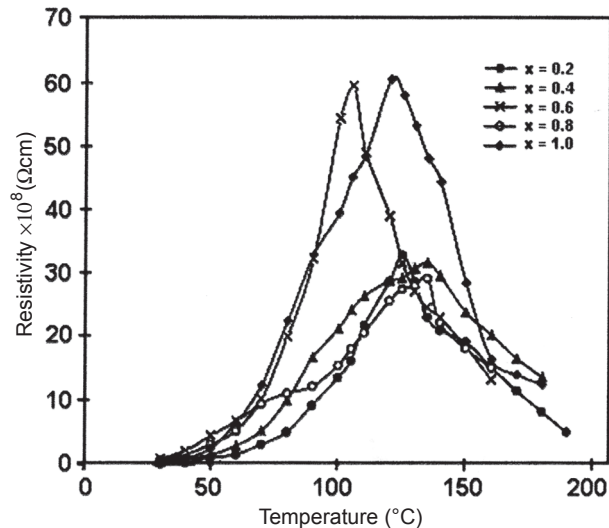
Figure 4. Temperature dependent D.C. resistivity of BSCLNN ceramics.

Table 3. Pyroelectric properties of BSCLNN solid solutions.

Li	$P_{RT}\times10^{-9}$ (C/cm² °C)	$P_{max}\times10^{-7}$ (C/cm² °C)	P_{Tc} (°C)	$FM_{RV}\times10^{-14}$ (CM/J)	$FM_{RN}\times10^{-12}$ (CM/J)	$FM_{RI}\times10^{-11}$ (CM/J)
0.2	0.92	1.51	197	1.14	0.26	0.59
0.4	0.79	1.79	198	1.19	0.24	0.51
0.6	1.05	1.61	202	1.86	0.35	0.69
0.8	1.13	1.80	197	1.30	0.31	0.75
1.0	1.21	1.85	191	1.54	0.34	0.78

the variation of resistivity with temperature. A graph is drawn between log ρ and $1/T$ for each sample and from the slope of the obtained straight line, the activation energies are calculated by using the following relation:

$$2.3026 \ \frac{dy}{dx} = \frac{E_a}{K} \tag{5}$$

(or)

$$E_a = 2.3026 \times K \times \frac{dy}{dx} \tag{6}$$

where E_a is the activation energy, K = Boltzman con-stant having the value 8.61×10^{-5} eV and dy/dx is the slope of the line.

The Ce doped BSLNN compositions show positive resistivity behavior (PTCR effect). The values of ρ_{RT} of Ce^{3+}-BSLNN is in the order of 10^7 Ωcm, and the value of ρ_{max} at anomaly temperature is in the order of 10^{10} Ωcm, and is three orders larger when compared with ρ_{RT}. This rise in ρ_{max} may be due to the presence of Ce^{3+} and Li^+ in these compositions. The maximum resistivity values are in the order of 10^{10} Ωcm. It is also observed that the ρ_{max} values are less when compared with other rare-earth doped BSNN compositions [21]. The activation energies were calculated in both the regions and tabulated in Table 4.

Table 4. D.C. resistivity Studies of BSCLNN solid solutions.

Li	$\rho_{RT} \times 10^7$ (Ωcm)	$\rho_{max} \times 10^{10}$ (Ωcm)	Activation energy (eV)	
			$+E_a$	$-E_a$
0.2	0.37	0.32	0.2213	0.2069
0.4	2.8	0.31	0.2150	0.1965
0.6	8.0	0.59	0.2168	0.2091
0.8	6.1	0.29	0.2144	0.2077
1.0	4.3	0.60	0.2188	0.2075

CONCLUSIONS

BSCLNN ceramics exhibited a single-phase ortho-rhombic (mm^2) crystal structure. Substitution of Cerium in Barium indicates no change in the orthorhombic structure but effects the lattice parameters. It is observed that Ce^{3+} substitutes Ba^{2+} at A2-site while Li^+ substitutes both Sr^{2+} and Na^+ at A1-site in the BSCLNN tungsten bronze system. The rare-earth Ce^{3+} and alkali Li^+ influence on BSNN could be attributed to the difference in the ionic radii of the cations, respectively. There are two orders of magnitude rise in the values of pyroelectric coefficient (P_{max}) at P_{Tc} compared with P_{RT}. The optimum figure of merit of voltage responsivity ($FM_{RV} = 1.86 \times 10^{-14}$ CM/J) has been observed in $Li_{0.6}$, normalized detectivity ($FM_{RN} = 0.35 \times 10^{-12}$ CM/J) has been observed in $Li_{0.6}$ and current responsivity ($FM_{RI} = 0.78 \times 10^{-11}$ CM/J) has been observed in $Li_{1.0}$, respectively. The maximum resistivity

values are in the order of 10^{10} Ωcm. The Ce doped BSLNN compositions show positive resistivity behavior (PTCR effect) which could be suitable for pyroelectric and PTCR applications.

References

1. Giess E. A., Scott B. A., Burns G., O'Kane D. F., Segmiiller A.: J.Am.Ceram.Soc. *52*, 276 (1969).
2. Hornebecq V., Elissalde C., Porokhonskyy V., Bovtun V., Petzelt J., Gregara I., Maglione M., Ravez J.: J.Phys.Chem. Solids. *64*, 471 (2003).
3. Hitoshi O., Masaki I.: Mater. Chem. and Phys. *79*, 208 (2003).
4. Bo L., Jiancong B., Zhenhong L., Liang S.: J.Rare Earths. *25*, 643 (2007).
5. Zheng X. H., Chen X. M.: J.Mater.Res. *17*, 1664 (2002).
6. Glass A. M.: J.Appl.Phys. *40*, 4699 (1981).
7. Ho W. W., Hall W. F., Neurgaonkar R. R., Dewames R. E., Mim T. L.: Ferroelectrics *38*, 833 (1981).
8. Francombe M. H.: Acta Cryst. *13*, 131 (1960).
9. Nagata K., Yamamoto Y., Igarashi H., Okazaki K.: Ferro-electrics *38*, 853 (1981).
10. Lines M. E.: Glass A. M.: *Principle and applications of ferroelectric and related materials*, p. 625, Clarenden Press, Oxford 1977.
11. Keitsiro A.: J.Phys.Soc.Jpn. *41*, 880 (1976).
12. Singh K. S., Sati R., Choudhary R. N. P.: J.Mater.Sci.Lett. *11*, 788 (1992).
13. Shannigrahi S. R., Choudhary R. N. P., Atul K., Acharya H. N.: J.Phys.Chem.Solids. *59*, 737 (1998).
14. Choudhary R. N. P., Shannigrahi S. R., Singh N. K.: Bull. Mater.Sci. *6*, 975 (1999).
15. Palai R., Choudhary R. N. P., Tewari H. S.: J.Phys.Chem. Solids. *62*, 695 (2001).
16. Panigrahi A., Singh N. K., Choudhary R. N. P.: J.Phys. Chem.Solids. *63*, 213 (2002).
17. Zheng X. H., Chen X. M.: Solid.State.Commun. *125*, 449 (2003).
18. Neurgaonkar R. R., Nelson J. G., Oliver J. R., Cross L. E.: Mat.Res.Bull. *25*, 959 (1990).
19. Chandramouli K., Srinivas Reddy G., Ramam K.: J.Alloys. Compounds, doi:10.1016/j.jallcom.2008.02.022 (2008).
20. Sambasiva Rao K., Prasad T. N. V. K. V., Subramanyam A. S. V., Lee J. H., Kin J. J., Cho S. H.: Mat.Sci.&Engg. *B 98*, 279 (2003).
21. Sambasiva Rao K., Koteswara Rao, Viswarupachary P.: Proc. Nat. Acad. Sci. *69*, I (1991).